Available online at www.sciencedirect.com
SCIENCE DIRECT®
International Journal of Heat and Fluid Flow 24 (2003) 130–136
International Journal of HEAT AND FLUID FLOW
www.elsevier.com/locate/ijhff

Natural convection in a liquid-encapsulated molten semiconductor with a steady magnetic field

Jonathan F. Kuniholm, Nancy Ma *

Department of Mechanical and Aerospace Engineering, North Carolina State University, Campus Box 7910, Raleigh, NC 27695, USA

Received 23 April 2002; accepted 7 August 2002

Abstract

This paper treats the buoyant convection in a layer of boron oxide, called a liquid encapsulant, which lies above a layer of a molten compound semiconductor (melt) between cold and hot vertical walls in a rectangular container with a steady horizontal magnetic field B. The magnetic field provides an electromagnetic damping of the molten semiconductor which is an excellent electrical conductor but has no direct effect on the motion of the liquid encapsulant. The temperature gradient drives counter-clockwise circulations in both the melt and encapsulant. These circulations alone would lead to positive and negative values of the horizontal velocity in the encapsulant and melt, respectively, near the interface. The competition between the two buoyant convections determines the direction of the horizontal velocity of the interface.

1. Introduction

There are many fluid flows that occur during the growth of semiconductor crystals in magnetic fields. The physical understanding of these flows is key to the development of optimal electromagnetic (EM) crystal growth systems. Since molten semiconductors are excellent electrical conductors, the melt motion can be damped and controlled by a steady (DC) magnetic field in order to control the dopant distribution in the crystal, which depends on the convective and diffusive transport of the dopant in the melt. Electronic and optical devices are manufactured on single-crystal wafers sliced from ingots of semiconductor crystals. Since the performance of any device depends strongly on the uniformity of the local dopant concentration in the wafer on which it is produced, a major objective during the solidification of any semiconductor is to minimize dopant segregation in the crystal. With recent manufacturing advances, millions of devices are now produced on a single wafer, so that the need for a uniform dopant concentration in the wafer has dramatically increased. Recently, Walker and Ma (2002) have reviewed the literature on the use of magnetic fields during the bulk growth of semiconductor crystals.

During the magnetic liquid encapsulated Czochralski (MLEC) growth of compound semiconductor crystals, such as indium phosphide, phosphorus gas is bubbled at high pressure through an indium melt, and the indium and phosphorus fuse to form the compound InP. A layer of boron oxide (B_2O_3) encapsulates the melt to prevent escape of the volatile component (P). A single crystal seed is lowered through the encapsulant which initiates solidification and crystal growth begins in the presence of an externally applied magnetic field. This is an extremely important process because it was the first to produce 8 cm diameter twin-free indium phosphide crystals which was accomplished by using magnetic stabilization (Bliss et al., 1993). Morton et al. (2002) presented a model of dopant transport during the MLEC process. Previous researchers have investigated the effect of a steady magnetic field on buoyant convection in rectangular enclosures (Ozoe and Okada, 1989; Garandet et al., 1992; Alchaar et al., 1995). In particular, Garandet et al. (1992) and Alchaar et al. (1995) treated two-dimensional buoyant convection in a rectangular enclosure with a vertical magnetic field. Previous research which has treated systems that have liquid encapsulation have neglected any coupling between the

* Corresponding author. Tel.: +1-919-515-5231; fax: +1-919-515-7968.
E-mail address: nancy_ma@ncsu.edu (N. Ma).

0142-727X/02/$ - see front matter © 2002 Elsevier Science Inc. All rights reserved.
PII: S0142-727X(02)00205-9

buoyant convections in the molten semiconductor and in the liquid encapsulant and assumed that the liquid encapsulant is stagnant (Ma et al., 1998).

In the present paper, we investigate the coupling between the buoyant convection in the liquid encapsulant and in the molten semiconductor in a steady horizontal magnetic field in a model problem which captures the essential physical phenomena that occur in the coupling of the buoyant convections during MLEC crystal growth. Recent experiments (Riemann et al., 1996) have shown some very promising results with a steady horizontal magnetic field which is obtained by placing the crystal-growth furnace between the pole faces of an iron-yoke magnet. The magnetic field has an indirect effect on the buoyant convection in the boron oxide through the coupling of its motion through the encapsulant–melt interface. We investigate this coupling for a model problem in a rectangular geometry without solidification.

2. Problem formulation

This paper treats the two-dimensional buoyant convection in two layers of fluid with a molten semiconductor (melt) encapsulated by a layer of boron oxide in a steady horizontal or transverse magnetic field $\mathbf{B}\hat{\mathbf{x}}$. Here, $\mathbf{B}$ is the magnetic flux density while $\hat{\mathbf{x}}$ and $\hat{\mathbf{y}}$ are the unit vectors for the Cartesian coordinate system. Our dimensionless problem is sketched in Fig. 1. The coordinates and lengths are normalized by the length of the melt or boron oxide L, so that α and $(\gamma-\alpha)$ are the dimensionless depths of the melt and boron oxide, respectively. Along $x=0$ and 1, the liquids are maintained at temperatures T_c and T_h, respectively, where $T_h > T_c$. The boundaries at $y=0$ and γ are thermal insulators. Here, the fluid flows are driven by the temperature difference so that the characteristic velocities for the buoyant convection in the melt (Hjellming and Walker, 1987) and in the encapsulant are

$$U = \frac{\rho g \beta (\Delta T)}{\sigma B^2}, \tag{1a}$$

$$U_e = \frac{\rho_e g \beta_e (\Delta T) L^2}{\mu_e}, \tag{1b}$$

respectively, where $(\Delta T) = T_h - T_c$ is the characteristic temperature difference and g is gravitational acceleration. Here, ρ, β and σ are the density, thermal volumetric expansion coefficient and electrical conductivity of the melt while ρ_e, β_e and μ_e are the density, thermal volumetric expansion coefficient and dynamic viscosity of the encapsulant. We use the thermophysical properties of molten indium phosphide and boron oxide, as shown in Table 1. With $(\Delta T) = 50$ K and $L = 5$ cm (Farrell and Ma, 2002), the characteristic velocity in the encapsulant is $U_e = 0.014065$ m/s while the characteristic velocity in the melt is $U = 0.1571$, 0.006284 or 0.00006284 m/s for $B = 0.1$, 0.5 or 5 T, respectively.

The electric current in the melt produces an induced magnetic field which is superimposed upon the applied magnetic field produced by the external magnet. The characteristic ratio of the induced to applied magnetic field strengths is the magnetic Reynolds number, $R_m = \mu_p \sigma U L$, where μ_p is the magnetic permeability of the melt. For all crystal-growth processes, $R_m \ll 1$ and the additional magnetic fields produced by the electric currents in the melt are negligible.

In the Navier–Stokes equation for the melt, the characteristic ratio of the EM body force term to the inertial terms is the interaction parameter, $N = \sigma B^2 L/\rho U$, which varies as B^4. In the energy equation, the characteristic ratio of the convective to conductive heat transfer is the thermal Péclet number, $Pe_t = \rho c_p U L/k$, where c_p and k are the specific heat and thermal conductivity of the melt, respectively. For a sufficiently strong magnetic field, N is large and Pe_t is small, so that the inertial terms and the convective heat transfer terms are negligible. In a recent study, Ma and Walker (2001) investigated the roles of inertia and convective heat transfer on the buoyant convection during MLEC growth, and determined the errors associated with the

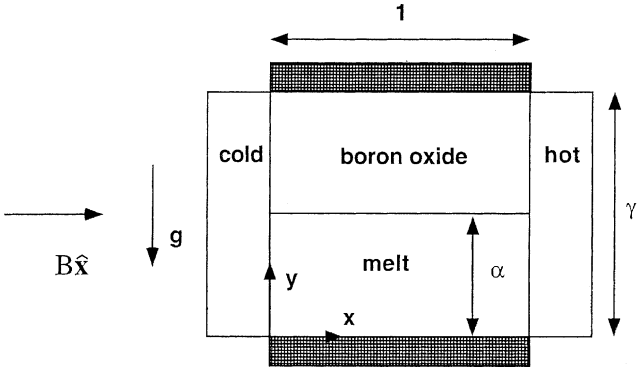

Fig. 1. Two-dimensional problem with a liquid encapsulant and molten semiconductor with a uniform, steady, horizontal magnetic field $\mathbf{B}\hat{\mathbf{x}}$ and with coordinates normalized by the distance between the hot and cold vertical walls.

Table 1
Thermophysical properties of molten InP and B_2O_3

Property	Molten InP	B_2O_3
Viscosity (Pa s)	8.19×10^{-4}	10
Density (kg/m^3)	5050	1530
Specific heat (J/kg K)	424	1864.3
Thermal conductivity (W/m K)	22.8	2.0
Thermal volumetric expansion coefficient (K^{-1})	4.44×10^{-4}	7.5×10^{-5}
Electrical conductivity (Ω^{-1} m^{-1})	7×10^5	0.0

neglect of inertial effects or of convective heat transfer for field strengths between 0.1 and 0.9 T. For MLEC growth of indium phosphide, they found that inertia and convective heat transfer significantly affect the buoyant convection when $B = 0.1$ T for which $N = 1.037$ and $Pe_t = 277.3$. As the magnetic field strength is increased from this value, the interaction parameter increases as B^4 and the thermal Péclet number decreases as B^{-2}, so that the ratios of the inertial force to the EM body force and of convective heat transfer to conductive heat transfer decrease. Ma and Walker (2001) found that the error due to neglect of inertial effects is only 2.7% for $B = 0.2T$ where $N = 16.59$ and $Pe_t = 69.33$, and is totally negligible for $B \geqslant 0.5$ T, while the error due to neglect of convective heat transfer is less than 4% for $B \geqslant 0.43$ T. Inclusion of inertia and convective heat transfer for weak magnetic field strengths is a straightforward extension of the present model, and will be included in future studies.

For the encapsulant, the characteristic ratio of the inertial force to the viscous force is the Reynolds number $Re = \rho_e U_e L/\mu_e$ and the characteristic ratio of the convective to conductive heat transfer is $Pe_{te} = \rho_e c_{pe} U_e L/k_e$, where c_{pe} and k_e are the specific heat and thermal conductivity of the encapsulant, respectively. For boron oxide, $Re = 0.108$ so that inertial terms are negligible. For boron oxide, the characteristic velocity based on our choice for the characteristic velocity U_e is $Pe_{te} = 1,003$. From our study, we find that the dimensionless velocities in the encapsulant are extremely small, i.e. they vary from roughly 10^{-6} to 10^{-5}, so that the effective thermal Péclet number is $Pe_{te,effective} = Pe_{te}|\mathbf{v}_e|_{max}$, where $|\mathbf{v}_e|_{max}$ is the maximum magnitude of the velocity in the encapsulant. Since $Pe_{te,effective} \ll 1$, convective heat transfer in the encapsulant is negligible.

The solutions for pure conduction are

$$T(\xi,\eta) = \frac{1}{2}(\xi+1) \quad \text{for } -1 \leqslant \xi \leqslant 1, \quad \text{and} \quad -1 \leqslant \eta \leqslant 1, \tag{2a}$$

$$T_e(\xi,\chi) = \frac{1}{2}(\xi+1) \quad \text{for } -1 \leqslant \xi \leqslant 1, \quad \text{and} \quad -1 \leqslant \chi \leqslant 1. \tag{2b}$$

where T is the deviation of the dimensional temperature in the melt from T_c normalized by (ΔT), and T_e is the deviation of the dimensional temperature in the encapsulant from T_c normalized by (ΔT). Here, $\xi = 2x - 1$ is the rescaled horizontal coordinate so that $-1 \leqslant \xi \leqslant +1$, while $\eta = -1 + 2y/\alpha$ and $\chi = (2y - \gamma - \alpha)/(\gamma - \alpha)$ are rescaled vertical coordinates so that $-1 \leqslant \eta \leqslant +1$ and $-1 \leqslant \chi \leqslant +1$. η corresponds to the vertical coordinate in the melt while χ corresponds to the vertical coordinate in the encapsulant.

For the present plane recirculating flow in the melt, the condition of zero net electric current in the z-direction implies that the electric field is zero (Hirtz and Ma, 2000). The only non-zero component of the electric current density, normalized by σUB, is given by Ohm's law, $j_z = -v$, where $\mathbf{v}(\xi,\eta) = u\hat{\mathbf{x}} + v\hat{\mathbf{y}}$ is the dimensionless velocity in the melt normalized by U.

For an inertialess flow, the buoyant convection in the molten semiconductor is governed by

$$\frac{\partial u}{\partial \xi} + \frac{1}{\alpha}\frac{\partial v}{\partial \eta} = 0, \tag{3a}$$

$$0 = -\frac{\partial p}{\partial \xi} + \frac{2}{Ha^2}\left(\frac{\partial^2 u}{\partial \xi^2} + \frac{1}{\alpha^2}\frac{\partial^2 u}{\partial \eta^2}\right), \tag{3b}$$

$$0 = -\frac{2}{\alpha}\frac{\partial p}{\partial \eta} - v + T + \frac{4}{Ha^2}\left(\frac{\partial^2 v}{\partial \xi^2} + \frac{1}{\alpha^2}\frac{\partial^2 v}{\partial \eta^2}\right), \tag{3c}$$

$$u = \frac{2}{\alpha}\frac{\partial \psi}{\partial \eta}, \quad v = -2\frac{\partial \psi}{\partial \xi}, \tag{3d}$$

where p is the deviation of the pressure from the hydrostatic pressure normalized by $\rho g \beta (\Delta T) L$, and ψ is the dimensionless streamfunction in the melt normalized by UL, while $-\mathbf{v}\hat{\mathbf{y}}$ is the EM body force due to the electric current in the z-direction and T in the buoyancy term is given by Eq. (2a). Here, the Hartmann number $Ha = \mathrm{BL}(\sigma/\mu)^{1/2}$ is the square root of the ratio of the EM body force to the viscous force, where μ is the dynamic viscosity of the molten semiconductor.

In an asymptotic solution for $Ha \gg 1$, the melt is divided into an inviscid core, Hartmann layers with an $O(Ha^{-1})$ thickness adjacent to the cold wall at $\xi = -1$ and the hot wall at $\xi = +1$, and parallel layers with an $O(Ha^{-1/2})$ thickness adjacent to the bottom wall at $\eta = -1$ and the encapsulant–melt interface at $\eta = +1$. The Hartmann layers have a simple, local, exponential structure, which matches any transverse core or parallel-layer velocities at $\xi = \pm 1$, which satisfies the no-slip conditions at the cold and hot walls, and which indicates that u in the core or parallel layer is $O(Ha^{-1})$ at $\xi = \pm 1$. Since the core carries O(1) flow, the flow circuit must be completed through two high-velocity parallel layers with $u = O(Ha^{1/2})$ and $v = O(1)$ inside these layers at $\eta = \pm 1$.

For an inertialess flow, the buoyant convection in the encapsulant is governed by

$$\frac{\partial u_e}{\partial \xi} + \frac{1}{(\gamma-\alpha)}\frac{\partial v_e}{\partial \chi} = 0, \tag{4a}$$

$$0 = -\frac{\partial p_e}{\partial \xi} + \frac{2}{Ha^2}\left[\frac{\partial^2 u_e}{\partial \xi^2} + \frac{1}{(\gamma-\alpha)^2}\frac{\partial^2 u_e}{\partial \chi^2}\right], \tag{4b}$$

$$0 = -\frac{2}{(\gamma-\alpha)}\frac{\partial p}{\partial \eta} + T_e + \frac{4}{Ha^2}\left[\frac{\partial^2 v_e}{\partial \xi^2} + \frac{1}{(\gamma-\alpha)^2}\frac{\partial^2 v_e}{\partial \chi^2}\right], \tag{4c}$$

$$u_e = \frac{2}{(\gamma-\alpha)}\frac{\partial \psi_e}{\partial \chi}, \quad v_e = -2\frac{\partial \psi_e}{\partial \xi}, \tag{4d}$$

where $\mathbf{v}_e(\xi,\chi) = u_e\hat{\mathbf{x}} + v_e\hat{\mathbf{y}}$ is the dimensionless velocity in the encapsulant normalized by U_e, p_e is the deviation of the pressure from the hydrostatic pressure normalized by $\mu_e U_e/L$, and ψ_e is the dimensionless streamfunction in the encapsulant normalized by $U_e L$, while T_e in the buoyancy term is given by Eq. (2b).

We apply the no-slip and no-penetration conditions along the walls at $\xi = -1, +1$, $\eta = -1$ and $\chi = +1$. For our flat interface, the no-slip and no-penetration conditions (Farrell and Ma, 2002) are

$$u(\xi+1) = \frac{\lambda_\beta}{\lambda_\mu} Ha^2 u_e(\xi,-1) \quad \text{for } -1 \leqslant \xi \leqslant +1, \tag{5a}$$

$$v(\xi,+1) = 0 \quad \text{for } -1 \leqslant \xi \leqslant +1, \tag{5b}$$

$$v_e(\xi,-1) = 0 \quad \text{for } -1 \leqslant \xi \leqslant +1. \tag{5c}$$

Here, $\lambda_\beta = \rho_e\beta_e/\rho\beta$ and $\lambda_\mu = \mu_e/\mu$. With boron oxide and molten indium-phosphide, $\lambda_\beta = 0.051177$ and $\lambda_\mu =$ 12,210. The stress is continuous across the interface (Farrell and Ma, 2002) so that

$$\frac{\partial u}{\partial y}(\xi,+1) = \lambda_\beta Ha^2 \frac{\partial u_e}{\partial y}(\xi,-1) \quad \text{for } -1 \leqslant \xi \leqslant +1. \tag{6}$$

Here we neglect gradients of the interfacial tension due to gradients of the temperature or of dopant concentration along the encapsulant–melt interface. A measure of the effects of interfacial tension gradients is the Marangoni number for the encapsulant, $Ma_e = \rho_e(-d\Gamma/dT)(\Delta T)L/\mu_e^2$, where Γ is the interfacial tension of the encapsulant–melt interface. There is no published data on the tension of an interface between a liquid semiconductor and boron oxide. If we use the values of Γ for a liquid-silicon free surface, which are certainly much larger than those for an encapsulant–melt interface, we find that $Ma_e = 0.00516$ for our typical process.

Eqs. (3a)–(6) were solved using a Chebyshev spectral collocation method with Gauss–Lobatto collocation points in ξ, η and χ. We use a sufficient number of collocation points to resolve the parallel layers near $\eta = \pm 1$ and to resolve the Hartmann layers at $\xi = \pm 1$. The number of collocation points in each direction in both the melt and the encapsulant were increased until the results were independent of these numbers. For example, when we used 21 collocation points in the ξ direction, 21 collocation points in the η direction in the melt, and 11 collocation points in the χ direction in the encapsulant with $\alpha = 0.3$ and $B = 0.1$ T, the minimum and maximum streamfunctions in the encapsulant are −0.0003839764 and 0.0, respectively while the minimum and maximum streamfunctions in the melt are 0.0 and 0.12624443, respectively. When we increased the resolution and used 41 collocation points in the ξ-direction, 41 collocation points in the η-direction in the melt, and 21 collocation points in the χ-direction in the encapsulant, the minimum value of the streamfunction in the encapsulant and the maximum value of the streamfunction in the melt changed by less than 0.0054% and 0.031%, respectively. Of course, the required number of collocation points increased as B was increased because the thickness of the boundary layers decreased and the velocity gradients increased.

3. Results

Prior to solidification in the liquid-encapsulated Czochralski process, the axisymmetric melt is entirely encapsulated by the boron oxide. After a single crystal seed initiates solidification and the crystal is pulled vertically upward, the encapsulant's depth increases and the melt's depth decreases due to solidification. Once the top of the crystal is pulled out of the encapsulant, the encapsulant's depth is constant while the melt's depth continues to decrease. The melt's depth decreases from an initial value of $\alpha = 0.6$ until the melt has disappeared. The purpose of the present paper is to illustrate the degree of coupling for various magnetic field strengths so we only present results for $(\gamma - \alpha) = 0.2666$ and for melt depths corresponding to the beginning of growth and the middle of growth, namely, $\alpha = 0.6$ and 0.3, respectively.

With the cold and hot walls at the left and right, respectively, the temperature gradient drives counterclockwise circulations in both the melt and the encapsulant. These circulations alone would lead to positive and negative values of u in the encapsulant and in the melt, respectively, near the interface. Therefore the shear stress σ_{xy} at the interface is always positive, i.e., a force to the left along the bottom of the encapsulant and an equal force to the right along the top of the melt. A positive value would reflect dominance by the encapsulant circulation, resulting in a clockwise circulation in the melt near the interface. A negative interfacial u would reflect dominance by the melt circulation, resulting in a clockwise circulation in the encapsulant near the interface. For all cases considered here except $B = 5$ T, the interfacial u is negative, which reflects dominance by buoyant convection in the melt, but this dominance decreases as the field strength is increased. For $B = 5$ T, the encapsulant has a slight dominance which drives a positive interfacial u.

For $\alpha = 0.6$, which corresponds to an early stage of growth, we present the dimensional interfacial shear stress for various magnetic field strengths in Fig. 2. For $B = 0.1$ T, the buoyant convection in the melt is relatively strong and produces a relatively large shear stress on the bottom of the encapsulant. As the magnetic field strength is increased, the magnitude of the buoyant

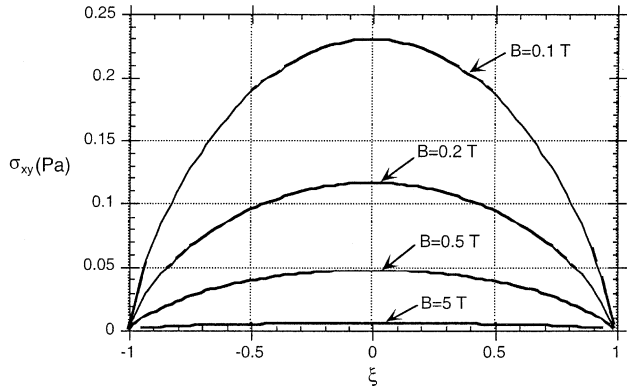

Fig. 2. Interfacial shear stress σ_{xy} versus ξ, for $\alpha = 0.6$ and $B = 0.1$, 0.2, 0.5 and 5 T.

convection in the bulk of the melt decreases roughly as B^{-2}, as reflected by our choice for the characteristic melt velocity in Eq. (1a). However, there is a jump in u across a high-velocity parallel layer with an $O(Ha^{-1/2})$ thickness adjacent to the encapsulant–melt interface, so that the interfacial shear stress decreases roughly as B^{-1} since the melt velocity in the parallel layer varies as $B^{-3/2}$ and the local y derivative varies as $B^{1/2}$. The effect of the EM damping is reflected in the dramatic decrease of the maximum magnitude of the melt's velocity for $\alpha = 0.6$ which is 0.3299 m/s for $B = 0.1$ T and 0.00003924 m/s for $B = 5$ T. For $\alpha = 0.3$, the maximum magnitude of the melt's velocity is 0.2283 m/s for $B = 0.1$ T and 0.00004736 m/s for $B = 5$ T.

For $\alpha = 0.6$ and $B = 5$ T, the maximum values of the streamfunctions in the melt and in the encapsulant are 0.1266 and 0.00002334, respectively, and the streamlines are plotted in Fig. 3a and b. For this strong field, there is a significant EM damping of the melt motion so that the maximum magnitude of the melt's dimensional velocity is 0.00004736 m/s which is 11.24 times the encapsulant's dimensional velocity. The buoyant convection in the encapsulant drives a positive interfacial velocity in the melt and a clockwise circulation inside the parallel layer along $\eta = +1$. That is, along $\eta = +1$, $u = +0.0642$ at $\xi = 0$ and decreases to $u = 0$ as $|\xi|$ approaches ± 1. The interfacial shear stress of the slow-moving melt decreases the velocity of the encapsulant but does not drive flow in the opposite direction.

For $\alpha = 0.6$ and $B = 1$ T, there is significantly less EM damping of the melt motion and the velocity of the melt is much larger. The interfacial shear stress is large enough to reverse some of the flow in the encapsulant, as reflected in Fig. 4 where the minimum and maximum values of the streamfunction are −0.0000012305 and 0.000010683, respectively, and the maximum value of the streamfunction in the melt is 0.1279. As shown in Fig. 2, the shear stress is largest at $\xi = 0$ and decreases to zero as $|\xi|$ increases so that the $\psi = -0.000001$ contour lies just above the middle of the interface. The

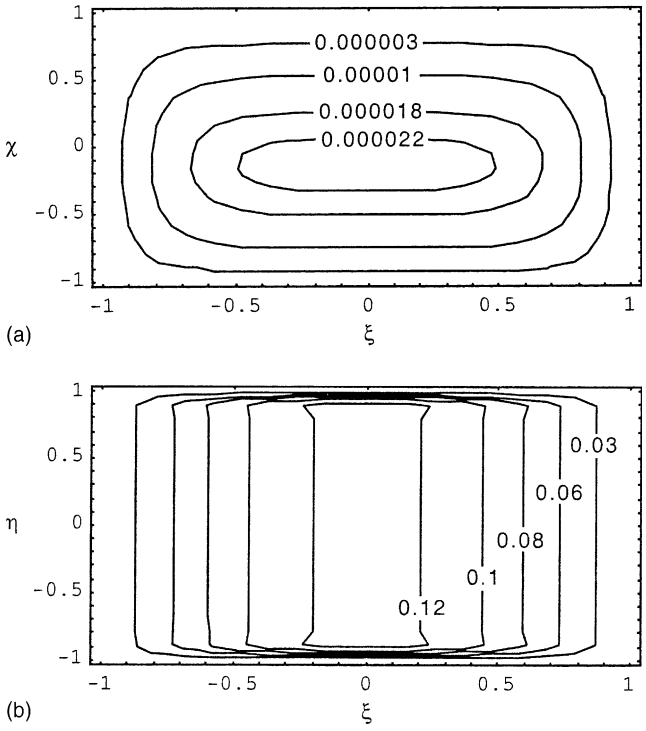

Fig. 3. Streamlines in the melt $\psi(\xi, \eta)$ and in the encapsulant $\psi_e(\xi, \chi)$ for $B = 5$ T: (a) $\psi(\xi, \eta)$, and (b) $\psi_e(\xi, \chi)$.

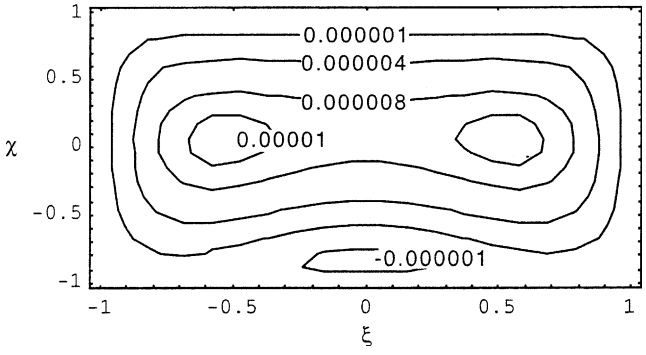

Fig. 4. Streamlines in the encapsulant $\psi_e(\xi, \chi)$ for $B = 1$ T.

circulation in the melt is entirely counter-clockwise with $u < 0$ along the interface. The maximum magnitude of the melt's velocity is 0.000001977 m/s and of the encapsulant's velocity is 0.003283 m/s.

For $\alpha = 0.6$ and $B = 0.5$ T, we present the streamlines in the encapsulant in Fig. 5, where the minimum and maximum values of the streamfunction are −0.00001735 and 0.0000030227, respectively, while the maximum value of the streamfunction in the melt is 0.1282. In Fig. 2, the curve for $B = 0.5$ T indicates that the shear stress has substantially increased, so that the clockwise circulation takes a major fraction of the encapsulant's volume. The maximum magnitude of the melt's velocity is 0.017027 m/s, which is 1799.5 times larger than that of the encapsulant. The maximum shear stress at $\xi = 0$ is

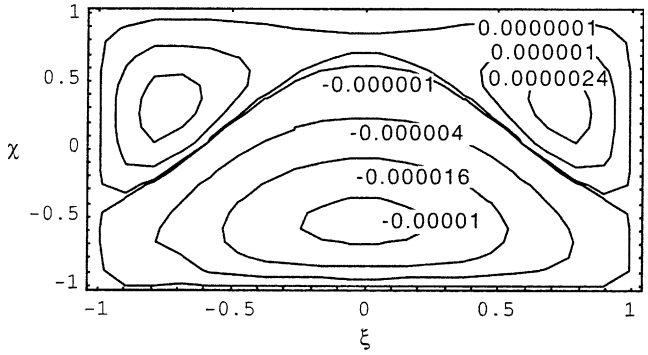

Fig. 5. Streamlines in the encapsulant $\psi_e(\xi,\chi)$ for $B = 0.5$ T.

causing the counter-clockwise circulations to decrease in strength and volume, so that the maximum value of the streamfunction in the encapsulant is smaller than for the strong field strengths and the circulations are pushed to the upper left and right corners of the encapsulant's volume, as reflected in Fig. 5.

For $\alpha = 0.6$ and $B = 0.1$ T, the minimum value of the streamfunction in the encapsulant is $\psi_{e,min} = -0.0001795$, and the maximum value of the streamfunction in the melt is 0.1260, as shown in Fig. 6. The large interfacial shear stress in Fig. 2 for $B = 0.1$ T causes all of the encapsulant's flow to reverse and its entire volume circulates in the clockwise direction, as shown in Fig. 6.

Since the magnitude of buoyant convection varies as α^{-1}, the maximum value of the velocity in the melt is smaller as crystal growth progresses. When the melt's volume has decreased to $\alpha = 0.3$, the shear stress has increased and a dominance by the encapsulant's circulation occurs with a larger value of B for $\alpha = 0.3$ than for $\alpha = 0.6$. That is, as we decrease the magnetic field strength from $B = 5$ T in increments of 1 T, the entire volume of the encapsulant circulates in the counter-clockwise direction until the field strength is $B = 2$ T with $\alpha = 0.3$ and $B = 1$ T with $\alpha = 0.6$ for which a small fraction of the encapsulant adjacent to the interface circulates in the clockwise direction. As the field strength is further decreased in increments of 0.1 T, an increasing fraction of the encapsulant flows in the clockwise direction until the clockwise circulation fills the entire volume at $B = 0.2$ T with $\alpha = 0.3$ for which $\psi_{e,min} = -0.00018099$ and at $B = 0.1$ T with $\alpha = 0.6$ for which $\psi_{e,min} = -0.00017948$.

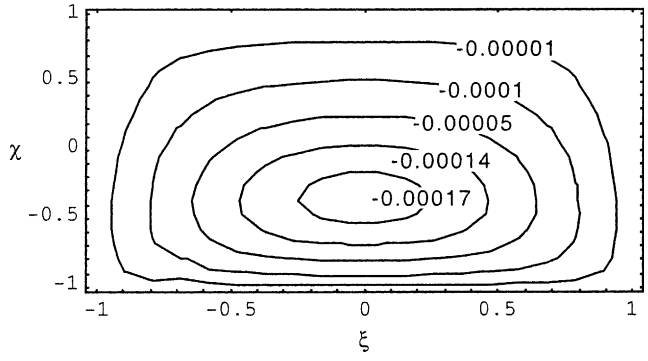

Fig. 6. Streamlines in the encapsulant $\psi_e(\xi,\chi)$ for $B = 0.1$ T.

4. Conclusions

The temperature gradient drives counter-clockwise circulations in both the melt and encapsulant. These circulations alone would lead to positive and negative values of the horizontal velocity in the encapsulant and melt, respectively, near the interface. The competition between the two buoyant convections determines the direction of the horizontal velocity of the interface. For $\alpha = 0.6$ and $B = 5$ T, there is significant EM damping of the melt motion and the encapsulant drives a positive interfacial velocity and a small clockwise circulation in the melt. For $\alpha = 0.6$ and a much weaker field $B = 0.1$ T, the maximum velocity in the melt is thousands of times larger than that of the encapsulant, thus causing nearly all the encapsulant to circulate in the clockwise direction.

Acknowledgements

This research was supported by the National Aeronautics and Space Administration under grant NAG8-1817. The calculations were performed on the IBM SP at the North Carolina Supercomputing Center in Research Triangle Park, NC.

References

Alchaar, S., Vasseur, P., Bilgen, E., 1995. Natural convection heat transfer in a rectangular enclosure with a transverse magnetic field. ASME Journal of Heat Transfer 117, 668–673.

Bliss, D.P., Hilton, R.M., Adamski, J.A., 1993. MLEK crystal growth of large diameter (1 0 0) indium phosphide. Journal of Crystal Growth 128, 451–456.

Farrell, M.V., Ma, N., 2002. Coupling of buoyant convections in boron oxide and a molten semiconductor in a vertical magnetic field. ASME Journal of Heat Transfer 124, 643–649.

Garandet, J.P., Alboussière, T., Moreau, R., 1992. Buoyancy driven convection in a rectangular enclosure with a transverse magnetic field. International Journal of Heat and Mass Transfer 35, 741–748.

Hirtz, J.M., Ma, N., 2000. Dopant transport during semiconductor crystal growth. Axial versus transverse magnetic fields. Journal of Crystal Growth 210, 554–572.

Hjellming, L.N., Walker, J.S., 1987. Melt motion in a Czochralski crystal puller with an axial magnetic field: Motion due to buoyancy and thermocapillarity. Journal of Fluid Mechanics 182, 335–368.

Ma, N., Walker, J.S., 2001. Inertia and thermal convection during crystal growth with a steady magnetic field. AIAA Journal of Thermophysics and Heat Transfer 15, 50–54.

Ma, N., Walker, J.S., Bliss, D.F., Bryant, G.G., 1998. Forced convection during liquid encapsulated crystal growth with an axial

magnetic field. ASME Journal of Fluids Engineering 120, 844–850.

Morton, J.L., Ma, N., Bliss, D.F., Bryant, G.G., 2002. Dopant segregation during liquid-encapsulated Czochralski crystal growth in a steady axial magnetic field. Journal of Crystal Growth 242, 471–485.

Ozoe, H., Okada, K., 1989. The effect of the direction of the external magnetic field on the three-dimensional natural convection in acubical enclosure. International Journal of Heat and Mass Transfer 32, 1939–1954.

Riemann, H., Lüdge, A., Hallman, B., Turschner, T., 1996. Growth of floating zone (FZ) silicon crystals under the influence of a transversal magnetic field. Proceedings of the 4th International Symposium on High Purity Silicon, Electrochemical Society Proceedings, vol. 96-13, pp. 49–57.

Walker, J.S., Ma, N., 2002. Convective mass transport during bulk growth of semiconductor crystals with steady magnetic fields. In: Tien, C.-L., Prasad, V., Incropera, F. (Eds.), Annual Review of Heat Transfer, vol. 12. Begell House, New York, pp. 223–263.